A Novel Approach for Finite Difference Treatment of Dielectric Interfaces in Photonics

Dušan Ž. Djurdjević[1]

***Abstract* – A general methodology that allows the derivation of high accurate finite difference (FD) formulas is presented. The methodology is made under a power series expansion of the transverse field components of the electromagnetic field. The use of derived FD formulas enables highly accurate modelling of dielectric interfaces and they have been validated in the electric field computations in electrostatics and full-vectorial waveguide simulation in photonics. Some illustrative results from full-vectorial waveguide eigenmode analysis in the frequency domain are presented.**

***Keywords* – Finite difference method, Helmholtz's equation, Numerical simulation, Photonics, Optoelectronics.**

I. INTRODUCTION

Amongst numerous techniques developed for solving partial differential equations, the finite difference method (FDM) is one of the most often-used numerical and simulation tool, [1]. FDM is ideally suited and often a favorite approach for CAD simulation software in microwaves, photonics (lightwave electromagnetics) and optoelectronics, because of its simplicity and flexibility.

In general, FDM technique appears in electromagnetics within two conceptually different approaches: the frequency domain FDM and the time domain FDM. Standard FDM usually refers to time and frequency independent problems described by Laplace's and Poisson's equations. FDM in the frequency domain is often-used approach in waveguide propagation numerical analysis in photonics, namely, as the finite difference beam propagation method (FD-BPM). Generally, the FD-BPM is a particular FDM technique in the frequency domain for the numerical finite difference solution of an exact vector Helmholtz's wave equation, [2], [3].

Standard FDM and the frequency domain FDM are usually implemented in a rectangular co-ordinate system. Certain restrictions arise when the FDM is applied to the structures with oblique or curved dielectric interfaces, because of the inevitable staircase approximation of the boundaries that occurs during the finite difference discretisation procedure. Many approaches have been proposed to improve the efficiency and accuracy of the FDM discretisation of the field near the dielectric interfaces. In area of optics engineering and research, those approaches are well known as the improved FD schemes, [4], [5].

In this paper, a new approach, which can be applied in standard FDM (electrostatics) and in frequency domain FD-BPM, in a uniform dielectric region, at a step-like dielectric interface of an arbitrary shape and near dielectric corner points, is presented. New FD-formulas are derived and used in numerical field calculations and BPM simulations. The results demonstrate the advantages and generality of the presented approach over standard and improved FD-approaches.

[1]Dušan Ž. Djurdjević is with the Faculty of Technical Sciences, Knjaza Miloša 7, 38220 Kosovska Mitrovica, Serbia, E-mail: drdusan.djurdjevic@gmail.com

II. OUTLINE OF THE METHOD

A. Theoretical Foundation – Helmholtz's wave equation

In linear and isotropic media, under the assumption that propagation is in perfectly insulating and z invariant media of refractive index n, in terms of the transverse electric field vector $\vec{\mathbf{E}}_\mathbf{t} = \vec{\mathbf{E}}_\mathbf{t}(x, y, z)$, Helmholtz's equation has a well known form, [2], [3],

$$\nabla^2 \vec{\mathbf{E}}_\mathbf{t} + k^2 n^2 \vec{\mathbf{E}}_\mathbf{t} = \nabla_t \left[\nabla_t \cdot \vec{\mathbf{E}}_\mathbf{t} - \frac{1}{n^2} \nabla_t (n^2 \vec{\mathbf{E}}_\mathbf{t}) \right], \quad (1)$$

where $k = \omega\sqrt{\varepsilon_0 \mu_0}$, $n = \sqrt{\varepsilon_r}$ and a differential operator ∇ is replaced as a sum of transverse and longitudinal part, $\nabla = \nabla_t + \nabla_z$. The similar equation can be derived for the transverse magnetic field vector $\vec{\mathbf{H}}_\mathbf{t}$.

The BPM is developed under paraxial approximation of Eq. (1), [2], [3]. Assuming that the forward traveling field of typical photonics waveguide-based structures has rapid phase variations along the guiding axis z and a slowly-varying vector envelope $\mathbf{E}_t$, one can rewrite Eq. (1) as,

$$j2kn_0 \frac{\partial \mathbf{E}_t}{\partial z} = \nabla_t \left[\frac{1}{n^2} \nabla_t (n^2 \mathbf{E}_t) \right] + k^2 (n^2 - n_0^2)\, \mathbf{E}_t, \quad (2)$$

where $j = \sqrt{-1}$, $\vec{\mathbf{E}}_\mathbf{t} = \mathbf{E}_t e^{-j\beta z} = \mathbf{E}_t e^{-jkn_0 z}$ and $\beta = kn_0$ is the background propagation constant with n_0 denotes a reference (modal) index. Eq. (2) is known as the paraxial full-vectorial approximation of Eq. (1).

In the 2D electrostatic approximation $(k \to 0,\ \partial/\partial z = 0)$, for the transverse vector $\vec{\mathbf{E}}_\mathbf{t} = \vec{\mathbf{E}}_\mathbf{t}(x, y)$, Eq. (1) simplifies to

$$\nabla_t \left[\frac{1}{n^2} \nabla_t (n^2 \vec{\mathbf{E}}_\mathbf{t}) \right] = 0, \quad (3)$$

where $n = \sqrt{\varepsilon_r}$. Eqs. (1), (2) and (3) contain a term,

$$\nabla_t \left[\frac{1}{n^2} \nabla_t (n^2 \mathbf{\Phi}_\mathbf{t}) \right], \quad (4)$$

where $\mathbf{\Phi_t}$ can be either vector $\vec{\mathbf{E}}_\mathbf{t}$ or slowly varying envelope vector $\mathbf{E_t}$. If n is a continuous function in the transverse plain (graded index cases), a differential term in Eq. (4) can be calculated analytically. However, if n is a discontinuous function (step-index cases), analytical solution is not possible, so there is a serious problem how to obtain consistent difference equations. The improved FD formulas approaches, [4], [5], take into account boundary conditions for the field and its derivatives near the dielectric interfaces. Approach presented in this paper improves FD-discretisation near step-like dielectric interfaces, but in a different, specific way, [6].

B. Derivation of FD-formulas, 2nd order of accuracy

Power series expansions of the electric field components as the functions of two Cartesian co-ordinates x and y are

$$E_x(x,y) = a_0 + a_1 x + a_2 y + a_3 x^2 + a_4 xy + a_5 y^2 + \cdots, \quad (5)$$

$$E_y(x,y) = b_0 + b_1 x + b_2 y + b_3 x^2 + b_4 xy + b_5 y^2 + \cdots. \quad (6)$$

In linear and isotropic source-free media, in the cases of 2D (xy) static field (e.g. electrostatics) and TEM field (e.g. transmission line field), from Maxwell's equations,

$$\frac{\partial E_x}{\partial x} + \frac{\partial E_y}{\partial y} = 0, \qquad \frac{\partial E_x}{\partial y} - \frac{\partial E_y}{\partial x} = 0, \quad (7)$$

we can evaluate power series expansion coefficients in Eqs. (5) and (6),

$$\mathbf{E}_x = a_0 + a_1 x + a_2 y + a_3 x^2 + a_4 xy - a_3 y^2 + \cdots, \quad (8)$$

$$\mathbf{E}_y = b_0 + a_2 x - a_1 y + \frac{a_4}{2} x^2 - 2a_3 xy - \frac{a_4}{2} y^2 + \cdots. \quad (9)$$

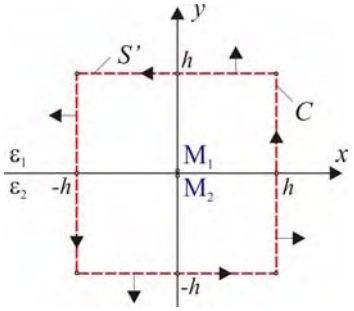

Fig. 1. Square 2D cell placed symmetrically at the interface of two dielectric media. Points M_1 and M_2 are placed close to interface. S' and C orientations are indicated with arrows.

If we assume that the dielectric interface has no charge, by applying the integral form of the Gauss' law on the Gaussian surface S (a contour S' in Fig. 1 is a cross-section of S in the transverse plane), and by using Eqs. (8) and (9), one can derive, [6],

$$\varepsilon_{r1} E_y\big|_{M_1} - \varepsilon_{r2} E_y\big|_{M_2} = \frac{h^2}{6}\left[\varepsilon_{r2}\frac{\partial^2 E_x}{\partial x\,\partial y}\bigg|_{M_2} - \varepsilon_{r1}\frac{\partial^2 E_x}{\partial x\,\partial y}\bigg|_{M_1}\right] + O(h^2). \quad (10)$$

By integrating electric field over contour C in Fig. 1, the similar formula to Eq. (10) can be obtained, [6],

$$E_x\big|_{M_1} - E_x\big|_{M_2} = \frac{h^2}{6}\left[\frac{\partial^2 E_y}{\partial x\,\partial y}\bigg|_{M_1} - \frac{\partial^2 E_y}{\partial x\,\partial y}\bigg|_{M_2}\right] + O(h^2). \quad (11)$$

When dielectric interface is arbitrary placed between two subsequent grid lines, integrations over S and C, Fig. 2, yield

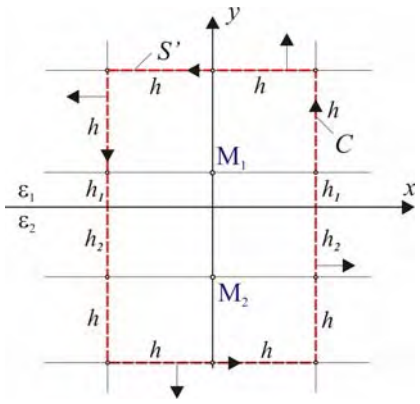

Fig. 2. Non-square 2D rectangular cell arbitrary placed at the interface of two dielectric media. Points M_1 and M_2 are placed at two subsequent grid lines.

$$\varepsilon_{r1} E_y\big|_{M_1} - \varepsilon_{r2} E_y\big|_{M_2} = \frac{h^2}{6}\left[(p_2 a_1 + q_2 a_4)_{M_2} - (p_1 a_1 + q_1 a_4)_{M_1}\right] + O(h^2), \quad (12)$$

and

$$E_x\big|_{M_1} - E_x\big|_{M_2} = \frac{h^2}{3}\left[(r_1 a_2 + s_1 a_3)_{M_1} - (r_2 a_2 + s_2 a_3)_{M_2}\right] + O(h^2). \quad (13)$$

In Eqs. (12) and (13) coefficients a_i, $i = 1, \cdots 4$, denote first and second derivatives of the field components in points M_1 and M_2, and coefficients p_i, q_i, r_i and s_i, $i = 1, 2$, are

$$p_i = -\varepsilon_{ri}\frac{6h_i}{h^2}, \quad q_i = \varepsilon_{ri}\left(1 - \frac{3h_i^2}{h^2}\right), \quad (14)$$

$$r_i = -\frac{6h_i}{h^2}, \quad s_i = \left(1 - \frac{3h_i^2}{h^2}\right). \quad (15)$$

In Eqs. (14) and (15), $h = \triangle = h_1 + h_2$ is a distance between two subsequent grid lines in the rectangular FD-mesh adopted, uniformly spaced both in x and y directions, Fig. 2.

C. Derivation of FD-formulas, 5th order of accuracy

Formulas given in Eqs. (10), (11), (12) and (13) are second order accurate. Formulas with higher order of accuracy can be derived in the similar way, by extending the order of power

series in Eqs. (5) and (6). The uniform rectangular grid scheme, in (x, y) co-ordinate system, used in derivation of the finite difference formulas near a dielectric interface, is shown in Fig. 3. The field components can be expanded in Eqs. (5) and (6) up to the 5th order, over the stencil diagramed in Fig. 3, resulting in 10 linear algebraic equations. Their solution yields FD-formulas for E_{x_0}, E_{y_0} and their derivatives with 5th order of accuracy. In Eqs. (16) to (21) 1st and 2nd derivatives are given only.

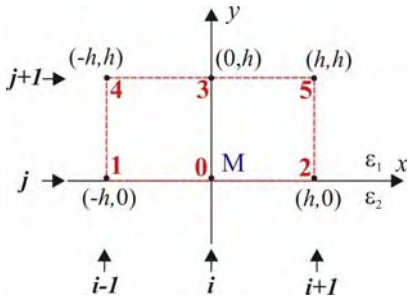

Fig. 3. Uniform rectangular scheme used in the finite difference formulas derivation. The point M is above the dielectric interface.

$$E_{x_0} = \frac{1}{10}[3E_{y_1} - 3E_{y_2} + 3E_{y_4} - 3E_{y_5} - (E_{x_1} + E_{x_2} - 10E_{x_3} - E_{x_4} - E_{x_5})] + O(h^5), \quad (16)$$

$$E_{y_0} = -\frac{1}{10}[3E_{x_1} - 3E_{x_2} + 3E_{x_4} - 3E_{x_5} + (E_{y_1} + E_{y_2} - 10E_{y_3} - E_{y_4} - E_{y_5})] + O(h^5), \quad (17)$$

$$a_1 = \frac{1}{10h}[(20E_{y_0} - 3E_{y_1} - 3E_{y_2} - 10E_{y_3} - 2E_{y_4} - 2E_{y_5}) + (E_{x_1} - E_{x_2} + E_{x_4} - E_{x_5})] + O(h^5), \quad (18)$$

$$a_2 = \frac{1}{10h}[(20E_{x_0} - 3E_{x_1} - 3E_{x_2} - 10E_{x_3} - 2E_{x_4} - 2E_{x_5}) - (E_{y_1} - E_{y_2} + E_{y_4} - E_{y_5})] + O(h^5), \quad (19)$$

$$a_3 = \frac{1}{4h^2}[(-10E_{x_0} + 2E_{x_1} + 2E_{x_2} + 4E_{x_3} + E_{x_4} + E_{x_5}) + (2E_{y_1} - 2E_{y_2} + E_{y_4} - E_{y_5})] + O(h^5), \quad (20)$$

$$a_4 = \frac{1}{2h^2}[-(10E_{y_0} - 2E_{y_1} - 2E_{y_2} - 4E_{y_3} - E_{y_4} - E_{y_5}) + (-2E_{x_1} + 2E_{x_2} - E_{x_4} + E_{x_5})] + O(h^5). \quad (21)$$

Similar FD-formulas can be derived for the stencils where the point M is set to be below, left and right to the dielectric interface. Combining those formulas with Eqs. (10) to (13) one can obtain FD formulas with high accuracy.

III. Numerical Results and Discussion

Performed test-computations in electrostatics have confirmed that derived finite FD formulas have truncation error proportional to the grid size, with the expected 5th order of accuracy. Some results obtained in simple FD-BPM test-simulations of buried waveguides are presented, [6].

The cross section of a simple buried dielectric waveguide is shown in Fig. 4. The most realistic cases - the full-vectorial real-axis and imaginary-axis beam propagation have been considered. The full-vectorial FD-BPM is adopted because of the presence of both transverse field components. Much simpler scalar and polarized formulations of Eq. (1) can not lead to the appropriate conclusions. Only TM propagation (E-field formulation) has been used in simulations.

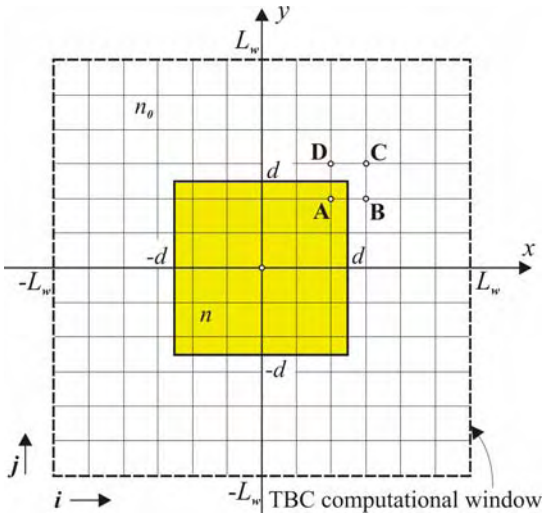

Fig. 4. Cross section of the buried waveguide. Dielectric interfaces are placed at the middle between two grid lines.

The numerical BPM simulation and the reference (modal) index evaluation are highly dependent on the electric field discretisation accuracy near the step-index interfaces. The approach presented in Section II is valid for the static and TEM fields. In TM propagation is $H_z = 0$, $\partial E_z/\partial z \cong 0$ (steady-state field regime), therefore the presented approach and derived FD-formulas can be used in TM case as well.

To avoid the influence of corners on the overall result, [7], FD-meshing in the transverse plane have been done by placing interfaces at the middle between two grid lines. For the field in points A, B, C and D, Fig. 4, the FD-formulas, with truncation error of order 3, have been derived and used:

$$E_{x_A} = E_{x\,i,j} = E_{x\,i-1,j-1} - E_{y\,i-1,j} + E_{y\,i,j-1} + O(h^3), \quad (22)$$

$$E_{y_A} = E_{y\,i,j} = E_{y\,i-1,j-1} + E_{x\,i-1,j} - E_{x\,i,j-1} + O(h^3), \quad (23)$$

$$E_{x_B} = E_{x\,i,j} = E_{x\,i+1,j-1} + E_{y\,i+1,j} - E_{y\,i,j-1} + O(h^3), \quad (24)$$

$$E_{y_B} = E_{y\,i,j} = E_{y\,i+1,j-1} - E_{x\,i+1,j} + E_{x\,i,j-1} + O(h^3), \quad (25)$$

$$E_{x_C} = E_{x\,i,j} = E_{x\,i+1,j+1} - E_{y\,i+1,j} + E_{y\,i,j+1} + O(h^3), \quad (26)$$

$$E_{y_C} = E_{y\,i,j} = E_{y\,i+1,j+1} + E_{x\,i+1,j} - E_{x\,i,j+1} + O(h^3), \quad (27)$$

$$E_{x_D} = E_{x\,i,j} = E_{x\,i-1,j+1} + E_{y\,i-1,j} - E_{y\,i,j+1} + O(h^3), \quad (28)$$

$$E_{y_D} = E_{y\,i,j} = E_{y\,i-1,j+1} - E_{x\,i-1,j} + E_{x\,i,j+1} + O(h^3). \quad (29)$$

In the uniform regions, the standard five-point FD formula has been used. A standard Crank-Nicolson algorithm has been used to simulate propagation in the z direction, and due to the well-confined waveguide field, transparent boundary conditions (TBC), [8], have been introduced at the edges of the computational window. For eigenmode solving, the imaginary distance BPM algorithm has been applied, [9].

TABLE I
CALCULATED MODAL INDEX AND CPU RUN-TIME USED IN IMAGINARY DISTANCE PROPAGATION

mesh size	$\triangle[\mu m]$	n_{ref}	$error_{rel.}$	CPU time
42×42	0.12500	1.222253	0.000727	00:01
82×82	0.06250	1.275934	0.000231	00:07
122×122	0.04166	1.274600	0.000125	00:22
162×162	0.03125	1.274077	0.000084	00:51
202×202	0.02500	1.271807	0.000063	01:36
242×242	0.02083	1.271645	0.000050	02:39
282×282	0.01785	1.271538	0.000041	05:04
322×322	0.01562	1.271462	0.000036	06:55
362×362	0.01389	1.271405	0.000031	09:50
402×402	0.01250	1.271361	0.000028	11:00

Numerical simulations have been performed for two different buried waveguide structures: low-index contrast one, with $n = 1.5$ $(\varepsilon_r = n^2 = 2.25)$, $2d = 1\,\mu$m, and the strong-index contrast waveguide, with $n = 3.4$ $(\varepsilon_r = 11.56)$, $2d = 0.5\,\mu$m. The wave-length has been kept at $\lambda = 1.5\,\mu$m in both cases. BPM step has been chosen to be $\triangle z = 0.1\,\mu$m, dimensions of the square computational domain have been truncated at $L_w = 2.5\,\mu$m in low, and at $L_w = 1.25\,\mu$m in strong-index contrast simulations.

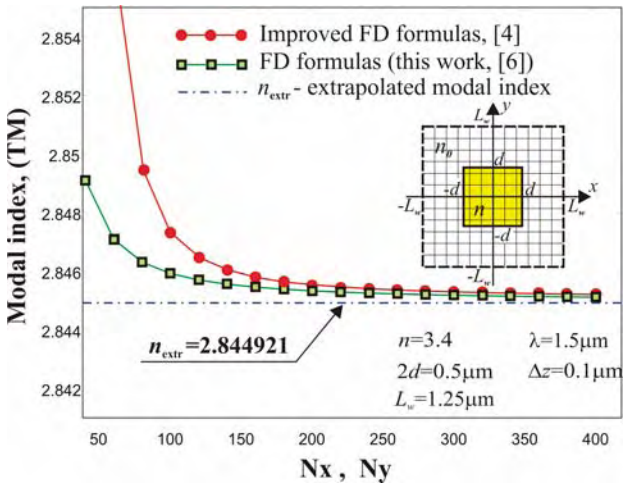

Fig. 5. Calculated modal index versus mesh size for waveguide shown in inset of Figure, strong-index contrast case.

Results for n_{ref} obtained in the imaginary distance BPM simulations in low-index contrast case are tabulated in Table I, together with data showing the total CPU use (in [min:s]) during the C++ code execution on PC (32-bit OS, 2.0 GHz) and the relative error computed against the extrapolated value for n_{ref} ($n_{ref_{extr.}} = 1.271301$, low-index contrast case, $n_{ref_{extr.}} = 2.844921$, strong-index contrast case). The CPU data represent the necessity of the accurate FD discretisation, since the mesh refinement implies a drastic increase in computer run-time.

The computed data for TM modal index n_{ref} versus number of grid lines in the x (N_x), and the y (N_y) directions, strong-index contrast case, are shown in Fig 5. Comparison with results obtained by using method published in [4], Fig. 5, shows that the present discretisation model demonstrates the faster convergence as the grid size is reduced. This result has been expected, as a consequence of the intrinsic property of the presented methodology enabling the true two-dimensional FD-discretising of the field near the dielectric interfaces and corners.

IV. CONCLUSION

The approach for finite difference treatment of dielectric interfaces has been presented. FD-formulas have been derived and applied to the electromagnetic field analysis and BPM simulations in photonics. Numerical simulations have been carried out to solve eigenmodes of TM mode field via the imaginary distance BPM for buried waveguide in the rectangular co-ordinate system, and results have been compared with those obtained from simulations based on previously reported improved FD algorithms. The flexibility of the approach, efficiency and accuracy of the derived FD-formulas recommends them for use in photonic CAD design.

REFERENCES

[1] C. Pozrikidis, *Numerical computation in Science and Engineering*, New York, Oxford University Press, 1998.

[2] C.L. Xu and W.P. Huang, "Finite-difference beam propagation method for guide-wave optics", PIER 11, pp. 1-49, 1995.

[3] T.M. Benson, D.Z. Djurdjevic, A. Vukovic and P. Sewell, "Towards numerical vector Helmholtz solutions in integrated photonics", In: Proc. IEEE on Transparent Optical Networks, vol. 2, pp. 1-4, 2003.

[4] Y.P.Chiou, Y.C. Chiang and H.C. Chang, "Improved three-point formulas considering the interface conditions in the finite-difference analysis of step-index optical devices", IEEE Journal of Lightwave Technology, vol. 18, no. 2, pp. 243-251, 2002.

[5] G.R. Hadley, "High-accuracy finite-difference equations for dielectric waveguide analysis I: Uniform regions and dielectric interfaces", IEEE Journal of Lightwave Technology, vol. 20, no.7, pp. 1210-1218, 2002.

[6] D.Z. Djurdjevic, "New finite-difference formulas for dielectric interfaces", Facta Universitatis (Niš), Ser.: Elec. Energ, vol. 23, no. 1, pp. 17-35, 2010.

[7] G.R. Hadley, "High-accuracy finite-difference equations for dielectric waveguide analysis II: Dielectric corners", IEEE J. of Lightwave Technology, vol. 20, no.7, pp. 1219-1231, 2002.

[8] G. R. Hadley, "Transparent boundary condition for beam propagation", Opt.Lett., vol.16, pp. 624-626, 1991.

[9] D.Yevick and B.Hermansson, "New formulations of the matrix beam propagation method: Application to rib waveguides", IEEE Journal of Quant. Elec., vol.25, pp. 221-229, 1989.